Surgical Oncology 28 (2019) 180–189

Contents lists available at ScienceDirect

Surgical Oncology

journal homepage: www.elsevier.com/locate/suronc

Overexpression of CLN3 contributes to tumour progression and predicts poor prognosis in hepatocellular carcinoma

Yu Xu[a,b,c,1], Huawei Wang[b,c,1], Yujian Zeng[a,b,c,1], Yan Tian[a,b,c,1], Zongwen Shen[b,c], Zhenrong Xie[b,c], Fengrong Chen[b,c], Liang Sun[a,b,c], Ruo Shu[a,b,c], Peng peng Li[a,b,c], Cheng Chen[a,b,c], Juehua Yu[b,c,***], Kunhua Wang[a,b,c,**], Huayou Luo[a,b,c,*]

[a] Department of Gastrointestinal and Hernia Surgery, The First Affiliated Hospital of Kunming Medical University, PR China
[b] Yunnan Clinical Center for General Surgery, The First Affiliated Hospital of Kunming Medical University, Kunming, Yunnan, 650032, PR China
[c] Yunnan Engineering Technology Centre for Digestive Disease, The First Affiliated Hospital of Kunming Medical University, Kunming, Yunnan, 650032, PR China

ARTICLE INFO

Keywords:
CLN3
Hepatocellular carcinoma
Tumour progression
Prognosis
Biomarker

ABSTRACT

The aberrant expression of ceroid-lipofuscinosis 3 (CLN3) has been reported in a variety of human malignancies. However, the role of CLN3 in the progression and prognosis of hepatocellular carcinoma (HCC) remains unknown. In this study, we found that CLN3 was frequently upregulated in HCC clinical samples and HCC-derived cell lines and was significantly correlated with an APF serum level ≥20 μg/L, a tumour size ≥5 cm, multiple tumours, and the absence of encapsulation. Kaplan-Meier showed that CLN3 upregulation predicted shorter recurrence-free survival (RFS) and overall survival (OS) time in HCC patients. Cox regression analysis revealed that CLN3 upregulation was an independent risk factor for RFS and OS. A functional study demonstrated that the knockdown of CLN3 expression profoundly suppressed the growth and metastasis of HCC cells both *in vitro* and *in vivo*. Mechanistic investigation revealed that the EGFR/PI3K/AKT pathway was essential for mediating CLN3 function. In conclusion, our results provide the first evidence that CLN3 contributes to tumour progression and metastasis and offer a potential prognostic predictor and therapeutic target for HCC.

1. Introduction

Hepatocellular carcinoma (HCC) is the fifth most common malignancy and the second leading cause of cancer-related deaths worldwide, and its incidence continues to rise [1,2]. Although the treatments for HCC have been greatly improved, the outcome of HCC is still unfavourable, with an approximately 30% overall 5-year survival rate after liver resection [3]. Although multiple tumour suppressor genes and oncogenes that participate in HCC development and progression have been identified [4,5], our knowledge of the cellular and molecular pathways underlying HCC progression remains limited. Therefore, it is necessary to elucidate the roles and action mechanisms of these genes in HCC growth, invasion and metastasis.

CLN3 is a recently identified defective gene in juvenile Batten disease, an inherited neurodegenerative childhood disease resulting from the accelerated apoptotic death of photoreceptors and neurons [6]. The CLN3 gene encodes a hydrophobic transmembrane protein, which is involved in intracellular trafficking and regulation in neuronal and non-neuronal cells [7–10]. Previous studies have indicated that CLN3 has anti-apoptotic properties in NT2 neuronal precursor cells and cancer cells [11,12]. In particular, previous studies have reported that CLN3 mRNA and protein are abundantly expressed in various cancer cell lines, including glioblastoma, neuroblastoma, and prostate, ovarian, breast and colon cancer [13,14]. In addition, a series of functional investigations have revealed that the knockdown of CLN3 by RNA interference (RNAi) inhibits proliferation and/or induces apoptosis in several cancer cells [13,14]. However, the potential role of CLN3 in HCC remains to be fully elucidated.

* Corresponding author. Department of Gastrointestinal and Hernia Surgery and Yunnan Institute of Digestive Disease, The First Affiliated Hospital of Kunming Medical University, 295 Xichang Road, Kunming, Yunnan Province, PR China. Tel.: 86 871 6532 4888; fax: 86 871 6533 6015.
** Corresponding author. Department of Gastrointestinal and Hernia Surgery and Yunnan Institute of Digestive Disease, The First Affiliated Hospital of Kunming Medical University, 295 Xichang Road, Kunming, Yunnan Province, PR China.
*** Corresponding author. Department of Gastrointestinal and Hernia Surgery and Yunnan Institute of Digestive Disease, The First Affiliated Hospital of Kunming Medical University, 295 Xichang Road, Kunming, Yunnan Province, PR China.
E-mail addresses: juehuayu@gmail.com (J. Yu), kunhuawang1@163.com (K. Wang), 1677546296@qq.com (H. Luo).
[1] These authors contributed equally to this work.

https://doi.org/10.1016/j.suronc.2018.12.003
Received 21 May 2018; Received in revised form 16 November 2018; Accepted 16 December 2018

Table 1
Clinical characteristics of the 192 HCC patients based on the protein level of CLN3.

Feature	CLN3		χ2	P-value
	High	Low		
All cases				
Age, y			0.508	0.559
≥55	54	36		
< 55	56	46		
Gender			0.187	0.665
Male	100	73		
Female	10	9		
HBsAg			0.45	0.837
Positive	96	68		
Negative	14	14		
AFP, μg/L			71.839	< **0.001**
≥20	66	8		
< 20	44	74		
Tumour size, cm			9.468	**0.002**
≥5	58	25		
< 5	52	57		
Tumour number			5.631	**0.018**
Single	36	30		
Multiple	74	52		
Vascular invasion			0.310	0.578
Absent	63	30		
Present	47	52		
Capsular formation			12.557	< **0.001**
Absent	95	53		
Present	15	29		
Liver cirrhosis			0.626	0.429
Absent	60	40		
Present	50	42		
Edmondson-Steiner grade			0.656	0.418
I-II	89	70		
III-IV	21	12		
BCLC Stage			0.051	0.821
A	42	30		
B+C	68	52		
TNM Stage			95.666	< **0.001**
I	110	30		
II-III	0	52		

The results were considered statistically significant at $P < 0.05$. Patients (n = 110) whose tumour tissue immunohistochemistry score (**strong** and **moderate**) were included in the high-expression group, and the remaining patients comprised the low-expression group Pearson's Chi-square tests were used for the correlation analysis between the expression levels of CLN3 and clinical features. The results were considered statistically significant at $p < 0.05$.

In the present study, we examined both the mRNA and protein expression levels of CLN3 in HCC-derived cell lines and clinical samples and analysed the correlation of CLN3 expression with clinicopathologic features and patient survival in an HCC cohort. In addition, we explored the potential role of CLN3 in the proliferation and metastasis of HCC cells ***in vitro*** and ***in vivo***. Our results provide the first evidence that increased CLN3 expression contributes to the aggressive behaviours of HCC cells and correlates with tumour progression and metastasis and may serve as an independent unfavourable prognostic indicator for HCC patients.

2. Materials and methods

2.1. Patients and specimens

The detailed clinicopathological characteristics of the patients are listed in Table 1. The time of the surgery was used to calculate the time to a given event. Overall survival (OS) was defined as the interval between surgery and the date of death. Recurrence-free survival (RFS) was defined as the interval between surgery and the date of recurrence. The OS and RFS were censored at the last follow-up visit (August 31, 2016) for surviving patients and those without recurrence. All patients (100%, 192/192) had a hepatitis B virus background. Micro-metastases were defined as tumours adjacent to the border of the main tumour that could only be observed under a microscope. Tumour differentiation was graded according to the Edmondson–Steiner grading system [15]. The tumour stage was defined according to the Barcelona Clinic Liver Cancer (BCLC) staging system [15]. An additional 50 HCC patients were recruited between January 1, 2011 and September 30, 2013, and their resected samples were subjected to RNA extraction for quantitative RT-PCR.

2.2. Real-time qPCR analysis

Real-time qPCR was performed as described previously [16]. Briefly, total RNA was isolated from frozen specimens or cell lines using TRIzol Reagent (Invitrogen). Reverse transcription (RT) was performed using the RevertAid™ First Strand cDNA Synthesis Kit (Fermentas) according to the manufacturer's instructions. After the RT reaction, the cDNA template was quantitated using real-time PCR technology. PCR was performed on an ABI Prism 7500 Sequence Detection System with SYBR Premix Ex Taq™ II (Takara) using the $2^{-\Delta\Delta CT}$method. Gene expression results were normalized to the internal control β-actin. The primers used in this study are as follows: CLN3 forward, 5′-GGTGGAC AGTATTCAAGGG-3′; reverse, 5′-CTTGGCAGAAAGACGAAC-3′; β-actin forward, 5′-AATCGTGCGTGACATTAAGGAG-3′; reverse, 5′-ACTGTGTT GGCGTACAGGTCTT-3′. Each sample was tested in duplicate.

2.3. Western blot analysis

Western blot assays were performed as described previously [17]. Briefly, tumour specimens or whole-cell extracts were prepared in lysis buffer [Tris-HCl (20 mM), pH 7.4, NaCl (150 mM), glycerol (10%), Nonidet P-40 (0.2%), EDTA (1 mM), EGTA (1 mM), PMSF (1 mM), NaF (10 mM), aprotinin (5 mg/mL), leupeptin (20 mM), and sodium orthovanadate (1 mM)] and centrifuged at 12,000 g for 30 min. The protein concentrations were measured using the BCA assay. Immunoblotting was performed using specific primary antibodies, and immunocomplexes were incubated with appropriate horseradish peroxidase-conjugated or fluorescein-conjugated secondary antibodies and then detected using an ECL kit (Santa Cruz Biotechnology) or an Odyssey fluorescence scanner (Li-Cor, Gene Company). β-actin was used as a loading control. The primary antibodies specific for CLN3, phospho-EGFR (p-EGFR), p-AKT, p-ERK1/2, total-EGFR (T-EGFR), T-AKT, T-ERK1/2 and PTEN were purchased from Abcam. The anti-β-actin antibody was purchased from Santa Cruz Biotechnology.

2.4. Immunohistochemistry

The immunohistochemistry of paraffin-embedded tissue sections was performed as described previously [16]. Briefly, the sections were deparaffinized and rehydrated. The endogenous peroxidase activity was blocked with 3% H_2O_2 for 10 min. Antigens were retrieved with citrate buffer (10 mM, pH 6.0) for 15 min at 100 °C in a microwave oven. After blocking, the sections were incubated with a primary anti-CLN3 antibody (Abcam, ab192473, 1:200) at 4 °C overnight in a moist chamber, followed by incubation with an anti-rabbit peroxidase-conjugated secondary antibody (Santa Cruz) at room temperature for 30 min. Finally, the visualization signal was developed with diaminobenzidine (Dako), and the slides were counterstained with haematoxylin. The stained sections were analysed by two experienced researchers. The immunohistochemistry score (IRS) mainly depended on the intensity of the staining. Representative images of the immunohistochemistry scores are shown in Fig. 1F, and the scoring results from four images of each tissue, which included two repetitions analysed by two researchers, were averaged in the last step. An IRS of moderate and strong

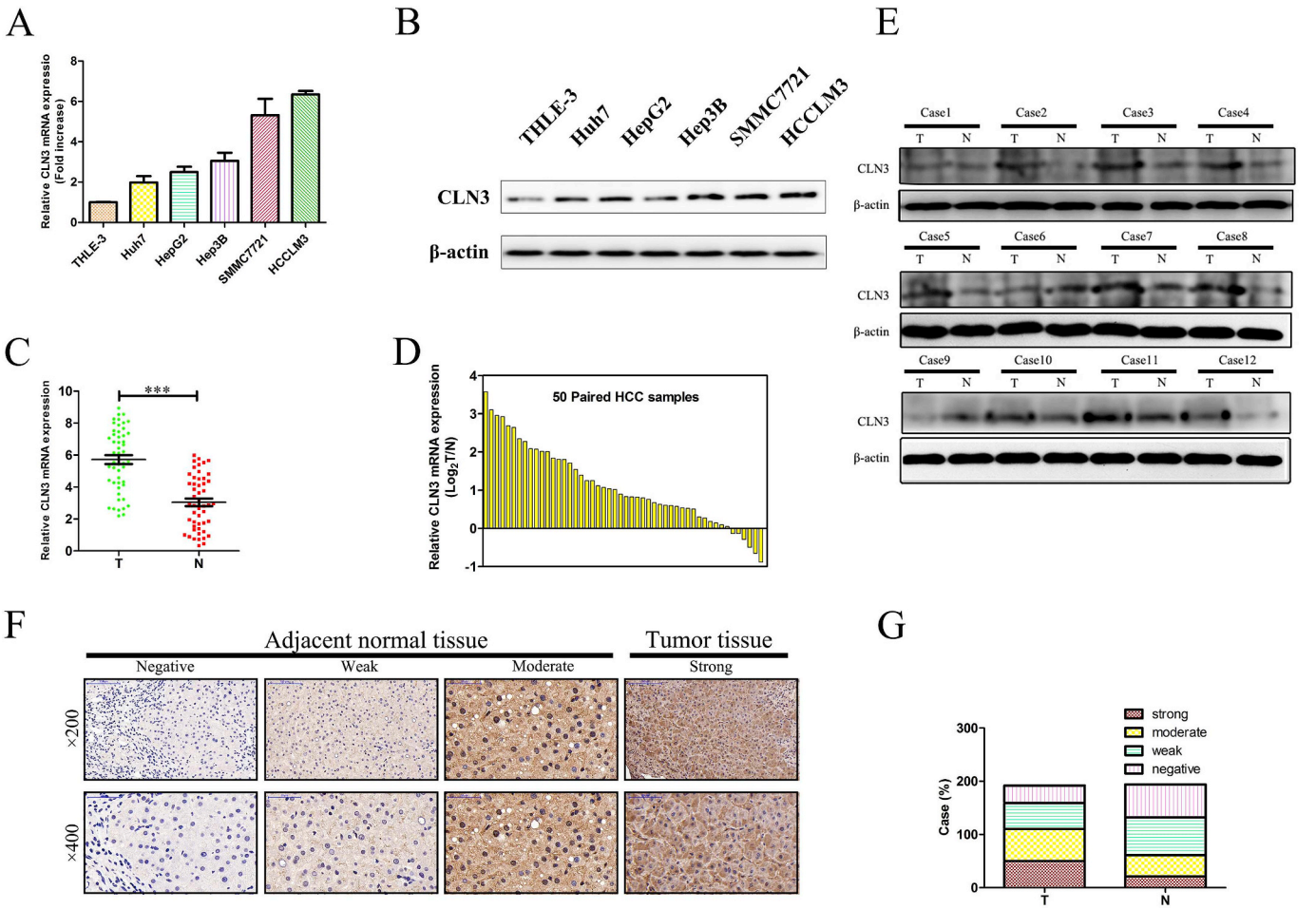

Fig. 1. Frequently increased expression levels of CLN3 in HCC cell lines and human HCC tissues. (**A**) Relative expression levels of CLN3 mRNA in THLE-3 and HCC-derived cell lines were determined by real-time qPCR. Gene expression results were normalized to the internal control β-actin. (**B**) Protein expression levels of CLN3 in THLE-3 and HCC-derived cell lines were determined by western blot assay. β-actin was used as a loading control. (**C–D**) Relative expression levels of CLN3 mRNA in 50 paired human primary HCC tissues and adjacent nontumour tissues were determined by real-time qPCR. Gene expression results were normalized to β-actin. (T, tumour tissues; N, adjacent nontumour tissues) (**E**) CLN3 protein expression in paired tumour and adjacent nontumour tissues was determined by western blot assay. (**F**) Representative immunohistochemical expression patterns of CLN3 in cancerous and adjacent normal mucosa tissues are shown. (Magnification, upper panel, × 200; lower panel, × 400) (**H**) Percentage of cases with different staining intensities of CLN3 in the tumour or adjacent nontumour tissues in the study cohort (*p < 0.05;**p < 0.01;***p < 0.001).

was used to define tumours with high CLN3 expression, and an IRS of (negative and weak) was used to indicate tumours with low CLN3 expression.

2.5. Reagents

Dimethyl sulfoxide (DMSO), crystal violet, the EGFR tyrosine kinase inhibitor AG1478 and the PI3K-specific inhibitor LY294002 were all purchased from Sigma-Aldrich.

2.6. Cell lines and cell culture

The indicated hepatocellular carcinoma cell lines (SMMC-7721, HCC-LM3, Huh7, HepG2, and Hep3B) and normal liver cell lines (THLE-3) were purchased from the Cell Bank of Type Culture Collection of Chinese Academy of Sciences (Shanghai, China). All cell lines were maintained at 37 °C in a humidified incubator containing 5% CO2 in Dulbecco's modified Eagle's medium (DMEM) or RPMI-1640 supplemented with 10% heat-inactivated foetal bovine serum and passaged every 2–3 days to maintain logarithmic growth.

2.7. Lentivirus infection and transient transfection

Lentiviral vectors containing human CLN3 short-hairpin RNA (shCLN3 1 or shCLN3 2) or scrambled non-targeting shRNA (Scramble) were prepared by the Genechem Company (Shanghai, China). A scramble non-targeting shRNA was used as a control. Lentivirus infection experiments were performed as described previously [16]. Briefly, the cells were infected with the indicated virus at a multiplicity of infection (MOI) of 10 in the presence of polybrene (8 mg/mL) for 8 h. Twenty-four hours later, the supernatant was replaced with fresh medium. After infection, stable colonies were selected in medium containing 3 μg/mL puromycin for 2–3 weeks. The expression of CLN3 in the infected cells was validated by qPCR and western blot assays. For plasmid transfection experiments, the cells were transiently transfected using PEI (Polyplus; AFAQ) as described previously [16], and the expression of AKT in the transfected cells was validated by western blot assay (Fig. S2).

2.7.1. Cell proliferation assay

The cell proliferation assay was performed using Cell Counting Kit-8 solution (Dojindo Laboratories) according to the manufacturer's instructions. Briefly, the cells were seeded at a density of 4×10^3/well

onto 96-well plates and treated with 10 μL/well of the Cell Counting Kit-8 solution, and the cell viability was measured at the indicated times. The optical density of the well was measured at 450 nm using a microplate reader.

2.8. Colony-formation assay

The cells were trypsinized to generate a single-cell suspension, and 500 cells/well were seeded onto 6-well plates. The dishes were returned to the incubator for 14 days, and the colonies were fixed with methanol for 1 h at room temperature and then stained with 0.5% crystal violet for an additional 1 h.

2.9. Cell migration and invasion assay

Migration and invasion assays were performed as described previously [16]. Briefly, the cells were trypsinized, centrifuged, and resuspended in serum-free medium followed by plating into the upper chamber at a density of 2×10^5/well. Complete medium (700 μL) was added to the lower chamber as a chemoattractant. After incubation for 16–18 h for the migration assay or 20–24 h for the invasion assay, the cells were fixed in methanol and stained with 0.1% crystal violet. The cells on the upper surface of the chamber were removed by wiping with a cotton swab, and migration and invasion were determined by counting the cells that migrated to the lower side of the chamber using a microscope at × 100 magnification. Six random microscopic fields were counted per chamber in each group, and these experiments were repeated at least three times.

2.10. In vivo xenograft and metastasis tumour assays

The xenograft tumour model was performed as described previously [16]. Briefly, six-week-old nude mice, purchased from the Animal Center of Kunming Medical University, were subcutaneously injected in the lateral flanks with the indicated cells at a density of 2×10^6. Tumour development was observed weekly with a calliper, and the tumour volume was calculated using the following formula: larger diameter × (smaller diameter) ^{2}/2. For the lung metastatic model, nude mice were injected through the tail vein with the indicated cells at a density of 1×10^6. The mice were sacrificed at ten weeks post injection. The lungs of each mouse were separated and fixed for **H&E** staining, and lung metastatic foci were detected under a microscope. All animals were housed in cages under standard conditions, and the animal experiments were conducted according to national and international guidelines and approved by the Kunming Medical University Care Facility.

2.11. Statistical analysis

The data are presented as the mean ± standard error of the mean (SEM) unless otherwise indicated. Pearson's chi-square test or Fisher's exact test was used to analyse the relationship between CLN3 expression and the clinicopathologic features. The Mann-Whitney *U* test was used to compare CLN3 levels between groups. Kaplan-Meier analysis with log-rank test was used to assess patient survival between subgroups. A Cox proportional hazards regression model was applied for the univariate and multivariate analysis of the effect of each variable on survival. The statistical significance of differences was determined using one-way ANOVA in multiple groups, with the Tukey-Kramer multiple comparison test for post hoc comparisons. A prognostic combination model was constructed using the significant variables from the Cox multivariate analysis. All statistical analyses were carried out using SPSS PASW Statistics 18.0 software (SPSS, Inc., Chicago, IL), and a p value < 0.05 was considered statistically significant.

3. Results

3.1. Frequently increased expression levels of CLN3 in HCC cell lines and human HCC tissues

We first examined the mRNA and protein expression levels of CLN3 in several human HCC-derived cell lines (SMMC-7721, HCC-LM3, Huh7, HepG2, and Hep3B) and the normal liver cell line THLE-3. Real-time quantitative polymerase chain reaction (qPCR) and western blot analyses revealed that both the mRNA and protein expression levels of CLN3 were markedly increased in all five HCC cell lines examined when compared to the THLE-3 cells (Fig. 1A and B). Then, we detected CLN3 mRNA expression in 50 paired primary HCC tissues and corresponding adjacent nontumour samples. The RT-PCR results showed that the relative expression of CLN3 mRNA was significantly higher in the cancerous tissues than in the adjacent non-cancerous tissues (Fig. 1C, **$p < 0.001$**), and 88% (44/50) of the HCC tissue specimens tested showed a higher expression level of CLN3 mRNA when compared to that in their matched non-cancerous counterparts (Fig. 1D). Similar results were also observed in the western blot analysis (Fig. 1E). To further determine the protein phenotypic expression patterns of CLN3 in HCC clinical samples, immunohistochemical analysis was performed in 192 paired paraffin-embedded HCC specimens. Each pair consisted of cancerous and adjacent non-cancerous tissues derived from the same patient. The representative immunostainings of CLN3 protein (**negative**, **weak**, **moderate**, **strong**) in HCC tissues are shown in Fig. 1F. The immunohistochemical data clearly showed that the immunoreactive score (IRS) values of CLN3 were significantly higher in tumour tissues, and positive staining for CLN3 was detected in 82.8% (159/192) of the cancerous samples. Among these samples, 26.0% (50/192), 31.3% (60/192) and 25.5% (49/192) of the cases showed strong, moderate, and weak staining for CLN3 protein, respectively. In striking contrast, among the adjacent normal mucosa tissues examined, 67.7% (130/192) of the cases showed positive staining, 36.5% (70/234) showed weak staining, 20.8% (40/192) showed moderate staining, and 10.4% (20/192) showed strong staining for CLN3 (Fig. 1G). These findings indicated that CLN3 expression is frequently upregulated in HCC.

3.2. CLN3 upregulation is associated with aggressive clinico-pathological traits

Next, we analysed the association between the protein level of CLN3 and the clinicopathological characteristics in the 192 patients cohort (Fig. 1F). The patients were divided into two groups according to differences in the immunohistochemistry scores of the tumour tissues. Patients with a tumour tissue immunohistochemistry score (moderate and strong) were assigned to the high-expression group (110 patients), and the remaining patients were assigned to the low-expression group (82 patients). We found that high CLN3 expression was more frequently observed in HCC patients with APF serum levels ≥ 20 μg/L ($P < 0.001$), tumour sizes ≥ 5 cm ($P = 0.002$), multiple tumours ($P = 0.018$), and the absence of encapsulation ($P < 0.001$) (Table 1). Collectively, these findings indicated that upregulated CLN3 expression may be linked to the malignant progression of HCC.

3.3. Relationship between CLN3 expression and HCC patient prognosis

We further analysed the association between the protein levels of CLN3 and the prognosis of HCC patients after hepatectomy. We found that the CLN3 high-expression group had significantly poorer RFS ($P < 0.001$, Fig. 2A) and poorer OS ($P < 0.001$, Fig. 2B). Subgroup analysis revealed that among patients with a tumour sizes < 5 cm (126 patients), the difference in RFS and OS between the CLN3 high- and low-expression groups still existed ($P < 0.001$, $P = 0.001$, Fig. 2C and D). Further analysis indicated that of the patients who were AFP-negative (118 patients, the CLN3 high-expression group had significantly

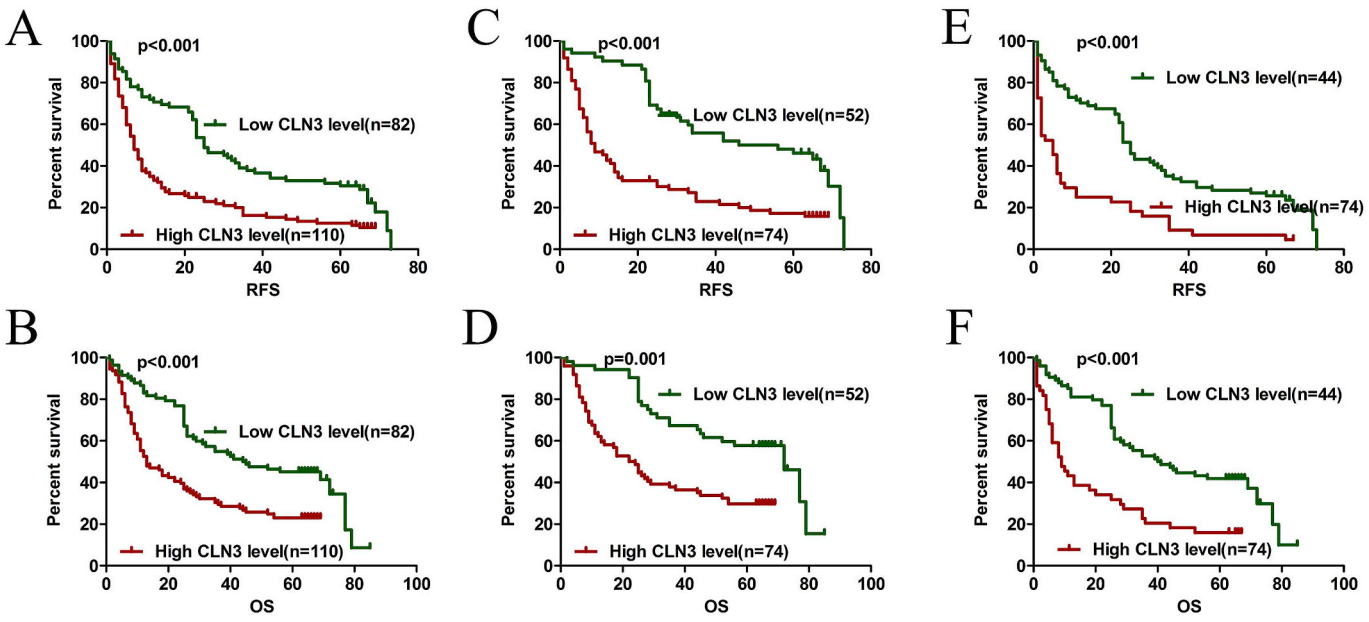

Fig. 2. Relationship between CLN3 expression and HCC patient prognosis. (**A** and **B**) Postoperative RFS and OS among all HCC patients. (**C** and **D**) Postoperative RFS and OS among HCC patients with a tumour size < 5 cm. (**E** and **F**) Postoperative RFS and OS among HCC patients with an AFP < 20 ng/μL. Statistical significance was assessed by two-sided log-rank tests (*p < 0.05;**p < 0.01;***p < 0.001).

Table 2
Multivariate analysis of the risk factors for RFS and OS.

Variable	RFS				OS			
	P	HR	95% CI		P	HR	95% CI	
Tumour diameter, > 5 cm vs. ≤5 cm	< 0.001	1.930	1.930	4.297	0.008	1.729	1.156	2.586
Tumour number, multiple vs. Negative	0.009	1.651	1.914	2.400	0.013	1.639	1.889	2.421
Microvascular invasion, Present vs. Absent	< 0.001	2.838	1.988	4.052	< 0.001	2.842	1.927	4.190
CLN3 expression, High vs. Low	0.025	1.484	1.051	2.095	0.025	1.550	1.056	2.277

poorer RFS (P < 0.001, Fig. 2E) and poor OS (P < 0.001, Fig. 2F). Univariate analysis indicated that among the clinicopathological characteristics, the CLN3 expression level, presence of microvascular invasion, tumour diameter ≥5 cm, multiple tumours, and the absence of capsule formation were correlated with RFS and OS (Table S1). Furthermore, multivariate Cox regression analysis indicated that the CLN3 expression level, presence of microvascular invasion, tumour diameter ≥5 cm, and multiple tumours were independent risk factors for RFS and OS in HCC patients (Table 2).

3.4. Knockdown of CLN3 suppresses the proliferation and tumour growth of HCC cells in vitro and in vivo

Given that increased CLN3 expression in HCC is a common molecular incident and correlated with aggressive tumour characteristics, we hypothesized that depletion of CLN3 can exert inhibitory effects on HCC development and progression. To test this hypothesis, we constructed stable CLN3-depleted cell models in two human HCC cell lines, SMMC7721 and HCCLM3, which have high levels of endogenous CLN3, using two lentivirus-mediated shRNAs targeting CLN3. The efficacy of the knockdown of CLN3 expression was confirmed by RT-PCR (Figs. S1A and S1B) and western blot analysis (Figs. S1C and S1D). The Cell Counting Kit-8 assay showed that the depletion of CLN3 resulted in a significant decrease in the proliferation rate in both SMMC7721 and HCCLM3 cells (Fig. 3A). In addition, CLN3 downregulation greatly impaired the colony-formation ability in each cell line (Fig. 3B). To verify the ***in vivo*** consequences of CLN3 knockdown, SMMC7721 control or CLN3-depleted cells were injected subcutaneously into the dorsal flank of nude mice, and tumour growth was monitored. As shown in Fig. 3C and D, the mice injected with CLN3-depleted cells showed significantly reduced xenograft tumour growth compared with those injected with control cells. These results indicate that CLN3 plays a positive role in HCC proliferation.

3.5. The knockdown of CLN3 inhibits the invasion and metastasis of HCC cells in vitro and in vivo

To determine the role of CLN3 in the motility of HCC cells, Transwell migration and Matrigel invasion assays were performed in CLN3-depleted and control cells. The Transwell migration assay demonstrated that silencing endogenous CLN3 expression markedly suppressed the migratory capabilities of SMMC7721 and HCCLM3 cells. Consistently, CLN3-silenced cells displayed significantly reduced invasive potential through Matrigel compared with the control cells (Fig. 4A and B). We further evaluated the effects of CLN3 downregulation on HCC cell metastasis ***in vivo*** using an experimental lung metastasis model. SMMC7721 control or CLN3-silenced cells were injected into the lateral tail vein of nude mice to induce lung metastasis. Ten weeks later, fewer and smaller micrometastatic lesions were detected microscopically in the lungs of mice inoculated with CLN3- depleted cells than in those of mice inoculated with control cells (Fig. 4C and D). Moreover, mice injected with CLN3-depleted cells had a significantly longer survival time compared with mice injected with control cells (Fig. 4E). Collectively, these findings suggest that CLN3 is essential for the invasive and metastatic potential of HCC cells both ***in vitro*** and ***in vivo***.

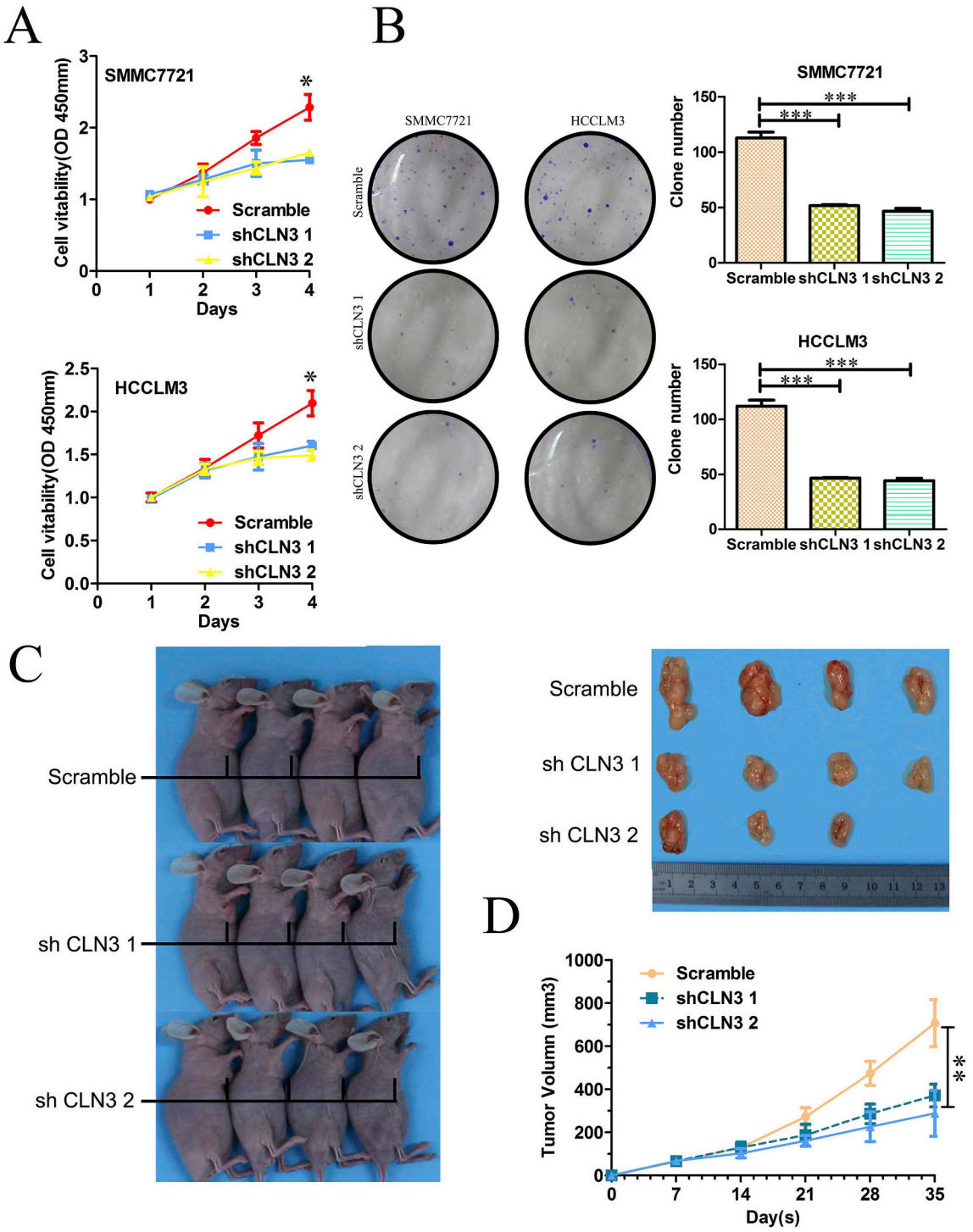

Fig. 3. Knockdown of CLN3 suppresses the proliferation and tumour growth of HCC cells *in vitro* and *in vivo*. (**A**) Cell viability of SMMC7721 or HCCLM3 cells infected with lentivirus expressing Scramble or shCLN3 1 or shCLN3 2 was determined by the Cell Counting Kit 8 assay. Plots are presented as the mean ± SEM of data from three independent experiments. (**B**) The effects of CLN3 knockdown on the proliferation of SMMC7721 or HCCLM3 cells were assessed by the colony-forming assay. Representative results are shown in the left panel. Plots in the right panel are presented as the mean ± SEM of data from three independent experiments. (**C**) Xenograft tumour model assays. SMMC7721 control or CLN3-depleted cells (2×10^6) were subcutaneously injected into the lateral flanks of nude mice. Subcutaneous xenografts from each group were excised from nude mice ($n = 4$). (**D**) The growth curves of xenograft tumour volumes. Plots are presented as the mean ± SEM (*p < 0.05; **p < 0.01; ***p < 0.001).

3.6. The EGFR/PI3K/AKT pathway plays a critical role in mediating CLN3 function

We next sought to explore the signalling mechanisms responsible for mediating the effects of CLN3 knockdown on cell growth and motility. Interestingly, the activation of EGFR was markedly suppressed in CLN3-depleted cells upon EGF stimulation (Fig. 5A). Additionally, the phosphorylation levels of AKT were also significantly decreased in CLN3-silenced cells compared with control cells in response to EGF stimulation. No substantial changes were observed in the levels of PTEN or

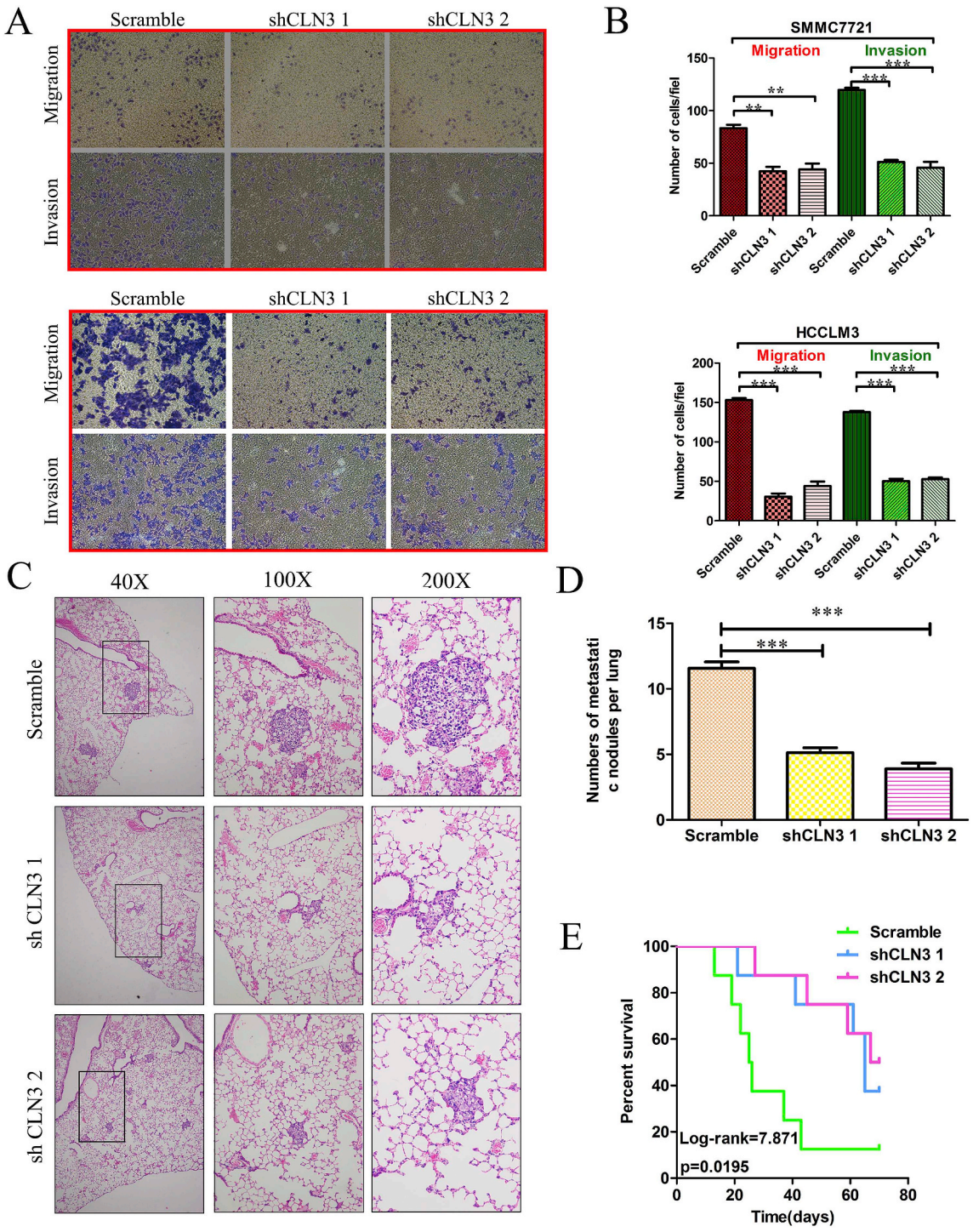

Fig. 4. Knockdown of CLN3 inhibits the invasion and metastasis of HCC cells *in vitro* and *in vivo*. (**A**) The effects of CLN3 knockdown on the migration and invasion of SMMC7721 or HCCLM3 cells were determined by the Transwell migration assay and Matrigel invasion assay, respectively. Representative results are shown. (**B**) Plots for panel A are presented as the mean ± SEM of data from three independent experiments. (**C**) Lung metastasis tumour model assays. A total of 1×10^6 SMMC7721 control or CLN3-depleted cells were injected into the tail vein of nude mice (n = 8). Ten weeks post inoculation, the mice were sacrificed, and metastatic tumour colonies in the lung were examined microscopically. Representative images of H&E staining of lung metastatic nodules in each group are shown. (Magnification, left panel, × 100; right panel, × 200) (**D**) The number of metastatic nodules in the lungs of each group is presented as the mean ± SEM. (**E**) Kaplan-Meier curves for overall survival of mice in each group. The p-value was determined using the log-rank test (*p < 0.05; **p < 0.01; ***p < 0.001).

ERK1/2 phosphorylation between CLN3-depleted and control cells. In addition, the pretreatment of cells with an EGFR-specific tyrosine kinase inhibitor (AG1478) not only effectively blocked the activity of EGFR but also eliminated the distinct activation of AKT signalling between CLN3-depleted and control cells, indicating that CLN3-mediated AKT activation occurs mainly downstream of EGFR activation (Fig. 5B). Importantly, the pretreatment of cells with AG1478 as well as LY294002, a specific inhibitor of PI3K, profoundly suppressed the proliferative and invasive potential of SMMC7721 cells and diminished the differences in the proliferation and invasion between CLN3-depleted and control cells (Fig. 5C and D). To further determine whether impaired AKT signalling is required for the CLN3 depletion-mediated

inhibition of HCC cell growth and invasion, SMMC7721 cells were transiently transfected with control vector or the myr-AKT (the constitutively active form of AKT) plasmid. As shown in Fig. 5E and F, activation of AKT signalling by the ectopic expression of myr-AKT significantly reversed the reduced tumour cell proliferative and invasive capabilities induced by CLN3 knockdown. These results reveal a critical role for the EGFR/PI3K/AKT pathway in the CLN3-facilitated growth and invasiveness of HCC cells.

4. Discussion

Hepatocarcinogenesis is a complex process characterized by increases in the expression of several factors that influence the survival of cancer cells by promoting cell proliferation and metastasis [18–20]. HCC is still one of the most dreadful human malignant diseases due to tumour recurrence and metastasis after surgical resection [21–25]. The histopathological and molecular features that lead to HCC initiation

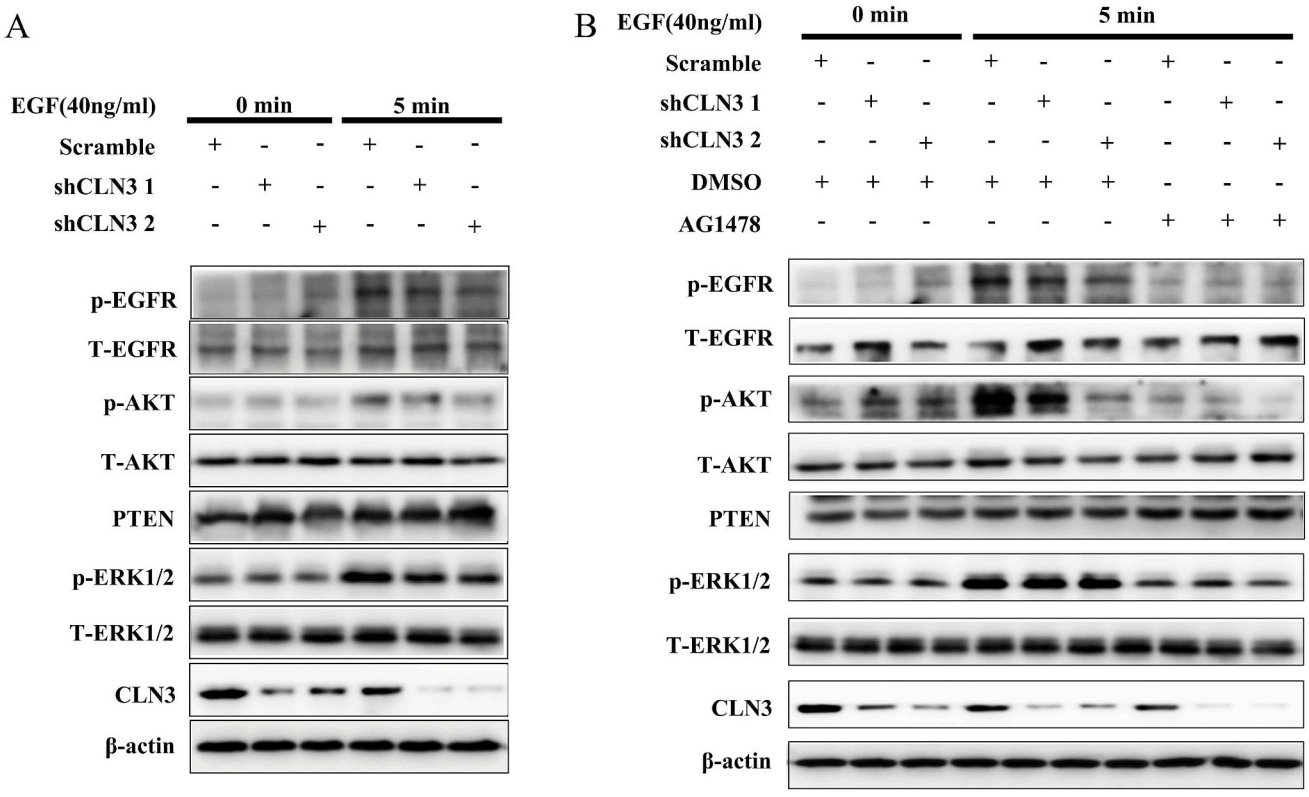

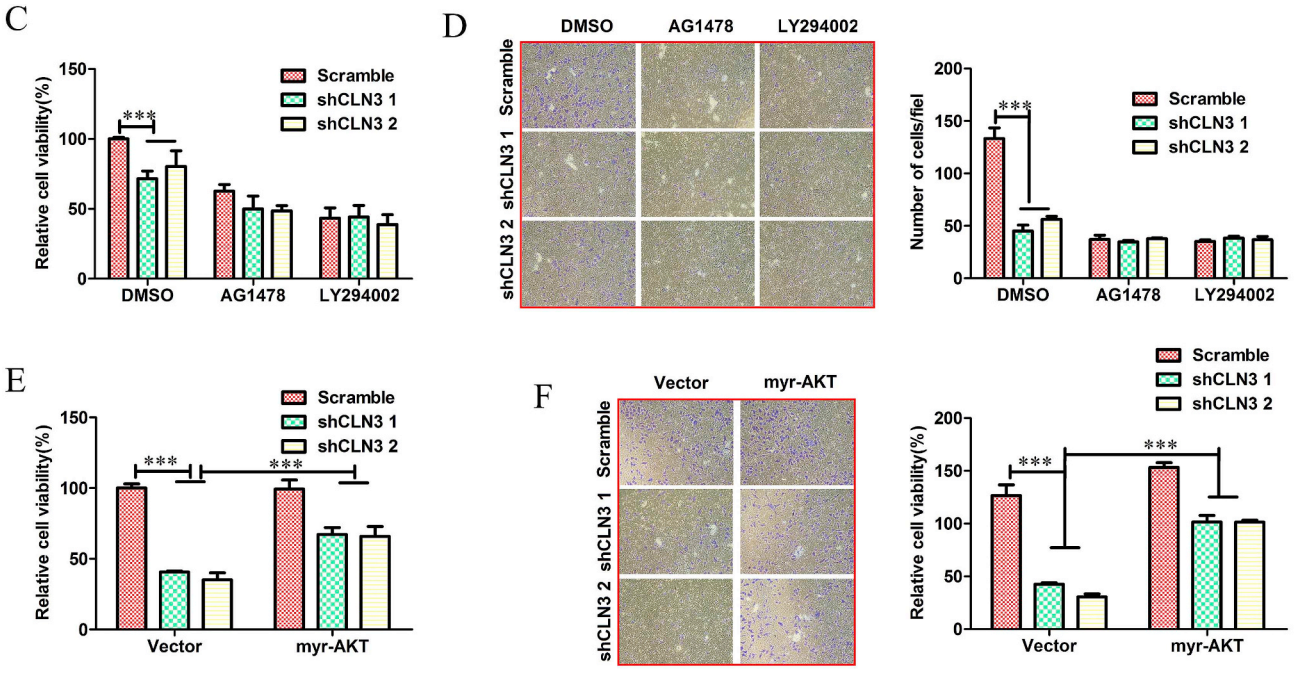

(caption on next page)

Fig. 5. EGFR/PI3K/AKT pathway plays a critical role in mediating CLN3 function. (**A**) SMMC7721 control or CLN3-depleted cells were serum starved overnight followed by treated with or without EGF (40 ng/mL) for 5 min, and then the cell lysates were harvested and subjected to western blot assay and probed with the indicated antibodies. (**B**) Indicated cells were serum starved overnight, followed by pre-incubation with DMSO or AG1478 (100 nM) for 2 h and then treatment with or without EGF (40 ng/mL) for 5 min. Cell lysates were harvested and subjected to western blot assay and probed with the indicated antibodies. (**C**) Indicated cells were pre-incubated with DMSO or AG1478 (100 nM) or LY294002 (10 μM) for 2 h and the cell viability was measured by Cell Counting Kit 8 assay at 72 h. Data are given as percentage of scramble lentivirus-infected DMSO-treated SMMC7721 cells as control which was set at 100%. Plots are presented as the mean ± SEM of data from three independent experiments. (**D**) Indicated cells were pre-incubated with DMSO or AG1478 (100 nM) or LY294002 (10 μM) for 2 h and then subjected to Matrigel invasion assays. Representative results are shown. Plots in the lower panel are presented as the mean ± SEM of data from three independent experiments. (**E**) Indicated cells were transiently transfected with control vector or myr-AKT (the constitutively active form of AKT) plasmid and the cell viability was measured by Cell Counting Kit 8 assay at 72 h. Data are given as percentage of scramble lentivirus-infected control vector-transfected SMMC7721 cells as control which was set at 100%. Plots are presented as the mean ± SEM of data from three independent experiments. (**F**) Indicated cells were transiently transfected with control vector or myr-AKT plasmid. Twenty-four hours post transfection, the cells were subjected to Matrigel invasion assays. Representative results are shown. Plots in the lower panel are presented as the mean ± SEM of data from three independent experiments (*$p < 0.05$;**$p < 0.01$;***$p < 0.001$).

and progression are still poorly understood [23–25]. Therefore, a better understanding of the molecular mechanisms underlying the pathogenesis of the disease is warranted to identify biomarkers for prediction and intervention.

In the present study, we reported that CLN3 protein expression was upregulated in HCC tissues and HCC-derived cell lines and was significantly correlated with several important clinicopathologic parameters, including tumour size ≥5 cm, absence of encapsulation, and vascular invasion. Higher expression of CLN3 protein predicted poorer RFS and OS and was an independent unfavourable prognostic indicator for HCC patients. Previous studies indicated that AFP-negative patients with tumour sizes < 5 cm are generally considered to have a better prognosis than AFP-positive patients with tumour sizes > 5 cm [26–29]; however, many of these patients still experience early disease recurrence and poor OS. Therefore, a precise biomarker for HCC is needed to predict the prognoses of patients with a smaller tumour size who are AFP negative. In our study, we found that within these populations, the high-expression group still had significantly poorer RFS than the low-expression group. Thus, the findings of the present study suggest that measuring CLN3 protein levels may enable clinicians to identify early stage disease patients who face a worse prognosis than other patients with early stage disease. Therefore, CLN3 may thus have prognostic value because it may allow clinicians to distinguish between early stage patients with a high risk of recurrence and early stage patients with a low risk of recurrence. The significant correlations between CLN3 expression in tumours and aggressive clinical behaviours and poor prognosis of HCC patients prompted us to investigate whether CLN3 plays a functional role in HCC progression and dissemination. Indeed, CLN3 knockdown markedly suppressed HCC growth and metastasis both ***in vitro*** and ***in vivo***. We further demonstrated that the EGFR/PI3K/AKT pathway was essential for mediating CLN3 action. Our results suggest a possible role for CLN3 in the development and progression of HCC.

EGFR and PI3K/AKT signalling have been implicated in the tumourigenesis, invasion and metastasis of cancer, including HCC [30–33]. Interestingly, we found that the knockdown of CLN3 markedly suppressed the phosphorylation levels of EGFR and AKT upon EGF stimulation and that the CLN3-dependent activation of AKT was mainly mediated through EGFR. This observation prompted us to further determine whether EGFR/PI3K/AKT signalling is involved in mediating the oncogenic property of CLN3 in HCC. As expected, the blockade of EGFR as activation and PI3K/AKT signalling by their respective pharmacological inhibitors eliminated the discrepant capacities in proliferation and invasion between control and CLN3-knockdown cells; conversely, the activation of AKT signalling by the ectopic expression of myr-AKT effectively reversed the inhibitory effects of CLN3 knockdown on HCC cell proliferation and invasion. Thus, our data reveal that CLN3 facilitates HCC progression, at least in part, through an EGFR/PI3K/AKT-dependent pathway. However, the mechanism by which CLN3 activates the EGFR/PI3K/AKT pathway and contributes to the pathogenesis and progression of HCC remains to be elucidated. Further studies are needed to validate the robustness of our findings before clinical translation and provide better insight into the molecular events involved in CLN3- mediated cancer progression and metastasis.

In summary, we report here, for the first time, that upregulated CLN3 expression correlates with the disease progression and unfavourable postoperative prognosis of patients with HCC. CLN3 plays a key role in HCC proliferation and metastasis and could be a useful prognostic biomarker for this malignancy. In addition to its prognostic value, our findings provide additional rationale for the potential utility of CLN3-targeted therapy in the treatment of HCC.

Conflicts of interest

The authors declare no conflicts of interest.

Acknowledgements

This work was supported by the National Natural Science Foundation of China (No. 81660094, No. 3171101074, No. 818170458, and No. 81860306).

Appendix A. Supplementary data

Supplementary data to this article can be found online at https://doi.org/10.1016/j.suronc.2018.12.003.

References

[1] M. Omata, L.A. Lesmana, R. Tateishi, P.J. Chen, S.M. Lin, H. Yoshida, M. Kudo, J.M. Lee, B.I. Choi, R.T.P. Poon, Asian Pacific association for the study of the liver consensus recommendations on hepatocellular carcinoma, Hepatology International 4 (2010) 439–474.
[2] A. Jemal, F. Bray, M.M. Center, J. Ferlay, E. Ward, D. Forman, Global cancer statistics, Ca - Cancer J. Clin. 61 (2011) 69–90.
[3] C. Bosetti, F. Turati, C.L. Vecchia, Hepatocellular carcinoma epidemiology, Best Pract. Res. Clin. Gastroenterol. 28 (2014) 753–770.
[4] H. Tsung-Hui, W. Chih-Chi, H. Chao-Cheng, C. Chao-Long, H. Chao-Hung, C. Chien-Hung, W. Jing-Houng, L. Sheng-Nan, L. Chuan-Mo, C. Chi-Sin, Down-regulation of tumor suppressor gene PTEN, overexpression of p53, plus high proliferating cell nuclear antigen index predict poor patient outcome of hepatocellular carcinoma after resection, Oncol. Rep. 18 (2007) 1417–1426.
[5] H.,. Ye, C. Zhang, B.-J. W, X.-H. T, W.-P. Z, Y.,. Teng, X. Yang, Synergistic function of Kras mutation and HBx in initiation and progression of hepatocellular carcinoma in mice, Oncogene 33 (2014) 5133–5138.
[6] T.I.B.D. Consortium, Isolation of a novel gene underlying batten disease, CLN3. Cell 82 (1995) 949–957.
[7] S.N. Phillips, J.W. Benedict, J.M. Weimer, D.A. Pearce, CLN3, the protein associated with batten disease: structure, function and localization, J. Neurosci. Res. 79 (2005) 573–583.
[8] D. Rakheja, S.B. Narayan, J.V. Pastor, M.J. Bennett, CLN3P, the Batten disease protein, localizes to membrane lipid rafts (detergent-resistant membranes), Biochem. Biophys. Res. Commun. 317 (2004) 988–991.
[9] D. Metcalf, A. Calvi, M. Seaman, H. Mitchison, D. Cutler, Loss of the batten disease gene CLN3 prevents exit from the TGN of the mannose 6-phosphate receptor, Traffic 9 (2010) 1905–1914.
[10] C. Andrea, T. Arianna, P. Giovanni, C.A. Galimberti, F. Pietro, M. Enrico, G. Gianpiero, C. Cristina, G. Gaetano, R. Ivana, Novel CLN3 mutation causing autophagic vacuolar myopathy, Neurology 82 (2014) 2072–2076.
[11] K.L. Puranam, W.X. Guo, W.H. Qian, K. Nikbakht, R.M. Boustany, CLN3 defines a novel antiapoptotic pathway operative in neurodegeneration and mediated by ceramide, Mol. Genet. Metabol. 66 (1999) 294–308.

[12] S.B. Narayan, D. Rakheja, J.V. Pastor, K. Rosenblatt, S.R. Greene, J. Yang, B.A. Wolf, M.J. Bennett, Over-expression of CLN3P, the Batten disease protein, inhibits PANDER-induced apoptosis in neuroblastoma cells: further evidence that CLN3P has anti-apoptotic properties, Mol. Genet. Metabol. 88 (2006) 178–183.
[13] S.N. Rylova, A. Andrea, P.S. Dixie-Ann, G. Wei-Xing, C. Jerry, P.J. Jansen, A.D. Proia, B. Rose-Mary, The CLN3 gene is a novel molecular target for cancer drug discovery, Cancer Res. 62 (2002) 801–808.
[14] X. Zhu, Z. Huang, Y. Chen, J. Zhou, S. Hu, Q. Zhi, S. Song, Y. Wang, D. Wan, W. Gu, Effect of CLN3 silencing by RNA interference on the proliferation and apoptosis of human colorectal cancer cells, Biomed. Pharmacother. 68 (2014) 253–258.
[15] H.B. El–Serag, K.L. Rudolph, Hepatocellular carcinoma: epidemiology and molecular carcinogenesis, Gastroenterology 132 (2007) 2557–2576.
[16] H. Chen, L. Hu, Z. Luo, J. Zhang, C. Zhang, B. Qiu, L. Dong, Y. Tan, J. Ding, S. Tang, A20 suppresses hepatocellular carcinoma proliferation and metastasis through inhibition of Twist 1 expression, Mol. Canc. 14 (2015) 186.
[17] L. Hu, L. Chen, L. Li, H. Sun, G. Yang, Y. Chang, Q. Tu, M. Wu, H. Wang, Hepatitis B virus X protein enhances cisplatin-induced hepatotoxicity via a mechanism involving degradation of Mcl-1, J. Virol. 85 (2011) 3214.
[18] F.Q. Wu, T. Fang, L.X. Yu, G.S. Lv, H.W. Lv, D. Liang, T. Li, C.Z. Wang, Y.X. Tan, J. Ding, ADRB2 signaling promotes HCC progression and sorafenib resistance by inhibiting autophagic degradation of HIF1α, J. Hepatol. 65 (2016) 314–324.
[19] W. Wen, T. Han, C. Chen, L. Huang, W. Sun, X. Wang, S.Z. Chen, D.M. Xiang, L. Tang, D. Cao, Cyclin G1 expands liver tumor-initiating cells by Sox 2 induction via Akt/mTOR signaling, Mol. Canc. Therapeut. 12 (2013) 1796–1804.
[20] T. Han, D.M. Xiang, W. Sun, N. Liu, H.L. Sun, W. Wen, W.F. Shen, R.Y. Wang, C. Chen, X. Wang, PTPN11/Shp2 overexpression enhances liver cancer progression and predicts poor prognosis of patients, J. Hepatol. 63 (2015) 651–660.
[21] K.A. Lee, J.Y. Ahn, S.H. Lee, S.S. Singh, D.G. Kim, J. Min, Y.H. Kim, Aptamer-based sandwich assay and its clinical outlooks for detecting lipocalin-2 in hepatocellular carcinoma (HCC), Sci. Rep. 5 (2015) 10897.
[22] H.B. El-Serag, F. Kanwal, Epidemiology of hepatocellular carcinoma in the United States: where are we? Where do we go? Hepatology 60 (2014) 1767–1775.
[23] H.B. El-Serag, Epidemiology of viral hepatitis and hepatocellular carcinoma, Gastroenterology 142 (2012) 1264–1273 e1261.
[24] H. Nie, X. Liu, Y. Zhang, T. Li, C. Zhan, W. Huo, A. He, Y. Yao, Y. Jin, Y. Qu, Specific N-glycans of hepatocellular carcinoma cell surface and the abnormal increase of core-α-1, 6-fucosylated triantennary glycan via N-acetylglucosaminyltransferases-IVa regulation, Sci. Rep. 5 (2015) 16007.
[25] C.H. Wang, Z.Y. Guo, Z.T. Chen, X.T. Zhi, D.K. Li, Z.R. Dong, Z.Q. Chen, S.Y. Hu, T. Li, TMPRSS4 facilitates epithelial-mesenchymal transition of hepatocellular carcinoma and is a predictive marker for poor prognosis of patients after curative resection, Sci. Rep. 5 (2015).
[26] D. Li, T.S. Mallory, AFP-L3: A new generation of tumor marker for hepatocellular carcinoma, Clin. Chim. Acta 313 (2001) 15–19.
[27] K. Shiraki, K. Takase, Y. Tameda, M. Hamada, Y. Kosaka, T. Nakano, A clinical study of lectin-reactive alpha-fetoprotein as an early indicator of hepatocellular carcinoma in the follow-up of cirrhotic patients, Hepatology 22 (2010) 802–807.
[28] H. Imamura, Y. Matsuyama, E. Tanaka, T. Ohkubo, K. Hasegawa, S. Miyagawa, Y. Sugawara, M. Minagawa, T. Takayama, S. Kawasaki, Risk factors contributing to early and late phase intrahepatic recurrence of hepatocellular carcinoma after hepatectomy, J. Hepatol. 38 (2003) 200–207.
[29] N.B. Ha, N.B. Ha, A. Ahmed, W. Ayoub, T.J. Daugherty, E.T. Chang, G.A. Lutchman, G. Garcia, A.D. Cooper, E.B. Keeffe, Risk factors for hepatocellular carcinoma in patients with chronic liver disease: a case-control study, Cancer Causes Control 23 (2012) 455–462.
[30] X. Fu, H. Wen, L. Jing, Y. Yang, W. Wang, X. Liang, K. Nan, Y. Yao, T. Tian, MicroRNA-155-5p promotes hepatocellular carcinoma progression by suppressing PTEN through the PI3K/Akt pathway, Cancer Sci. 108 (2017) 620–631.
[31] Q. Xu, X. Liu, Z. Liu, Z. Zhou, Y. Wang, J. Tu, L. Li, H. Bao, L. Yang, K. Tu, MicroRNA-1296 inhibits metastasis and epithelial-mesenchymal transition of hepatocellular carcinoma by targeting SRPK1-mediated PI3K/AKT pathway, Mol. Canc. 16 (2017) 103.
[32] J. Samarin, V. Laketa, M. Malz, S. Roessler, I. Stein, E. Horwitz, S. Singer, E. Dimou, A. Cigliano, M. Bissinger, PI3K/AKT/mTOR-dependent stabilization of oncogenic far-upstream element binding proteins in hepatocellular carcinoma cells, Hepatology 63 (2016) 813–826.
[33] Z. Wang, Q. Lei, B. Deng, S. Xing, S. Wu, J. Liao, J. Fan, Z. Peng, STYK1 promotes epithelial-mesenchymal transition and tumor metastasis in human hepatocellular carcinoma through MEK/ERK and PI3K/AKT signaling, Sci. Rep. 6 (2016) 33205.